

Induction of Hepatocellular Carcinoma in Conventional Domestic Swine Using N-Diethylnitrosamine and Phenobarbital

Angela Giselvania ^{1,2}, Vetrizah Juniantito ³, Heri Wibowo ⁴, Trifonia Pingkan Siregar ⁵, Soehartati Gondhowiardjo ²

¹Doctoral Program in Biomedical Sciences, Faculty of Medicine Universitas Indonesia, Jakarta, Indonesia; ²Department of Radiation Oncology, Faculty of Medicine Universitas Indonesia, Dr Cipto Mangunkusumo Hospital, Jakarta, Indonesia; ³Division of Pathology, School of Veterinary Medicine and Biomedical Sciences, IPB University, Bogor, Indonesia; ⁴Department of Parasitology, Faculty of Medicine Universitas Indonesia, Jakarta, Indonesia; ⁵Department of Radiology, Faculty of Medicine Universitas Indonesia, Dr Cipto Mangunkusumo Hospital, Jakarta, Indonesia

Correspondence: Soehartati Gondhowiardjo, Department of Radiation Oncology, Faculty of Medicine, Universitas Indonesia, Dr Cipto Mangunkusumo Hospital, Jl. Pangeran Diponegoro No. 71, Kota Jakarta Pusat, DKI, Jakarta, 10430, Indonesia, Email gondhow@gmail.com

Purpose: Large animal models are still used in many studies because of their likeness to humans. It has not been documented that regular-sized conventional farm-breed pigs, generally bred for meat production, can be used to generate hepatocellular carcinoma (HCC) animal models. The goal of this study was to investigate how N-diethylnitrosamine (DNA) and phenobarbital (PB) together can generate HCC in ordinary farmed pigs.

Materials and Methods: Conventional domestic swine (*Sus scrofa domesticus*) were used. DNA 15 mg/kg was intraperitoneally injected weekly for 12 weeks, while PB tablets (4 mg/kg) were also administered through food for 16 weeks. Blood testing and ultrasonography evaluation were performed to monitor the progress. Subsequently, computed tomography was conducted in cases with suspected nodules, followed by histopathological examination to confirm the diagnosis.

Results: Ten swine (seven males, three females; age: 2 months; weight: 9–15 kg) were included in the study and followed up for 25 months; nine were experimental, and one was control for ethical considerations. The maximum weight of animals during this study reached 162–228 kg. The weight gain seen in the intervention swine was predominantly lower than that documented in the control. The laboratory analysis revealed no notable abnormalities in liver function markers but did demonstrate statistically significant changes in urea ($p = 0.028$) and creatinine ($p = 0.003$) levels. Ultrasonography and computed tomography showed multiple liver nodules with characteristics resembling HCC. Serial imaging screening and more extended observations revealed that all animals eventually developed tumors. Histopathological confirmation at 15–22 weeks post-induction revealed that all intervened swine developed multiple nodules of well-differentiated HCC and some with hepatic angiosarcoma.

Conclusion: This study successfully generated HCC in conventional domestic swine with a DNA and PB combination. This investigation required at least 15 months to develop tumors. This model will be beneficial for future investigations of HCC in large animals.

Keywords: carcinogenesis, large animal model, hepatocellular carcinoma, domestic swine, DNA induction

Introduction

Hepatocellular carcinoma (HCC) accounts for >90% of liver cancer cases. Based on data from Global Cancer Statistics (GLOBOCAN) 2020, HCC is the second leading cause of cancer-related death worldwide.¹ Treatment options for HCC remain limited, and the results are unsatisfactory. Unfortunately, curative treatment (ie, resection or liver transplantation) is only possible for <20% of HCC cases. The majority of patients might undergo several locoregional treatments, such as radiofrequency ablation, transarterial chemoembolization, transarterial radioembolization, radiotherapy, and systemic therapy.² Moreover, the 5-year survival rate of patients remains <12%.³ Further investigation is warranted to improve the available treatment options for this disease. Establishing appropriate animal models for HCC is required for basic and translational studies, particularly those that can resemble human disease.

The development of animal models of HCC that are analogous to human disease is challenging, and research in this field is currently limited. Mouse models are a popular and convenient option for numerous experimental purposes. However, large-animal models are necessary for some studies, especially for the locoregional treatment of HCC (eg, radiation therapy, interventional radiology, and hyperthermia). These trials require an appropriate liver size, vasculature, and tumor microenvironment that mimic those of humans. This animal model may represent human HCC in terms of primary tumor and metastases, including intravascular invasion, simulation of the human tumor microenvironment, tumor-parenchymal cell response, and immune system response.

Currently, available animal models can be categorized as chemically induced, genetically engineered, and engrafted.⁴ Our animal models are chemically induced using N-diethylnitrosamine (DENa), a well-established substance that induces liver injury, and a genotoxic agent used for the chemical induction of HCC in models. In mice, DENa is typically used to induce liver cancer; however, it may also induce gastrointestinal, skin, respiratory, and hematopoietic tumors. The pathogenesis is caused by the alkylation of DNA structures that induces DNA damage and subsequent cell degeneration, as well as the production of reactive oxygen species through the activation of cytochrome P450 in hepatocytes.⁵ Moreover, Ho et al recently suggested that the administration of phenobarbital (PB) accelerates tumor formation. In a miniature pig model, PB shortened the time of tumor latency period from 10–26 months to 5–11 months.⁶ PB is a non-genotoxic promoter and a well-known inducer of drug-metabolizing enzymes that have been used in various rodent hepatocarcinogenesis model studies since it was first initiated by Weisburger et al in 1975.⁷ However, Ho et al were the first to utilize PB as an accelerator for HCC induction in large animal models, using miniature pigs.⁶ PB was demonstrated to activate CAR via an indirect mechanism. It is revealed that PB induces HCC carcinogenesis by increasing the CAR-Gadd45B complex that suppresses anti-tumor p38 MAPK activity.⁸

The induction of HCC into domestic swine could be further used in the field of oncology. In the field of radiotherapy, preclinical animal models are fundamental for understanding tumor and tissue response, thereby improving the therapeutic approach and treatment strategies in humans.⁹ This HCC induction experiment serves as the initial study for the spatially fractionated grid radiotherapy technique. This approach can be used to determine the molecular mechanism involved in the effects of these treatments. Currently, there is a lack of data regarding the DENa-induced liver carcinogenesis combined with PB in conventional domestic swine, especially in regular-sized conventional farm-breed swine, in terms of the latency period and rate of cancer development.

Materials and Methods

This study was conducted from January 2021 to March 2023 at the animal hospital and laboratories of the School of Veterinary Medicine and Biomedical Sciences, IPB University, Bogor, West Java, and at Cipto Mangunkusumo Hospital, Jakarta, Indonesia. All the experimental protocols and swine housing conformed to the Institutional Guidelines for Animal Care of the IPB University, as well as the Guide for Care and Use of Laboratory Animals: Eighth Edition by the National Research Council 2011. The Animal Ethics Committee Faculty of Veterinary Medicine and Biomedical Sciences, IPB University approved this study (approval number: 012/KEH/SKE/X/2020), the Board of the Faculty of Medicine, Universitas Indonesia (approval number: KET-371/UN2.F1/ETIK/PPM.00.02/2020) and Cipto Mangunkusumo Hospital (approval number: 03.02/2.2/641/2020).

Experimental Animals

Ten farm-breed domestic swine (*Sus scrofa domestica*) of mixed Landrace breeds, consisting of seven males and three females, aged two months and weighing 9–15 kg, were included in the study. All of the swine were maintained under observation for acclimatization before initiating the study. All subjects were fed twice daily with a standard diet of known composition and given access to water ad libitum.

To establish animal models of hepatocellular carcinoma (HCC), nine pigs were treated with DENa, and one healthy pig served as a negative control. This design was made to compromise between scientific rigor and minimizing the impact on the animal population while adhering to the 3Rs (replacement, reduction, and refinement) principles and ethical considerations. This compact design follows known ethical criteria and contributes to the development of useful HCC animal models for biological research.

Carcinogenic Agents

Nitrosamines, including DENA, are well-established acute hepatotoxins and carcinogens for the liver in men and numerous animals.⁵ Our study used the carcinogenic chemical DENA (N0756; Sigma–Aldrich, St. Louis, MO, USA) to stimulate the carcinogenesis process in the swine’s liver. DENA was intraperitoneally injected (dose: 15 mg/kg body weight) into the lower right quadrant of the abdomen weekly for 12 weeks.

To accelerate the process of carcinogenesis, PB (dose: 4 mg/kg body weight) was also added to the swine diet twice daily for five days per week, for a total of 16 weeks after DENA injection. The dosages of DENA and PB were calculated weekly depending on the body weight. DENA is sensitive to light; therefore, it was constantly maintained in the dark, and the substance was prepared in an indoor room to avoid direct exposure to sunlight. According to a previous study by Ho et al, who used minipigs as the model, tumor nodules were expected to develop within 5–11 months post-DENA and PB induction.⁶ Animal body weight measurements and laboratory and imaging tests were conducted regularly to monitor tumor growth.

Laboratory and Radiologic Evaluation

Blood testing, including a complete peripheral blood test, and evaluation of the levels of aspartate transaminase (AST) and alanine transaminase (ALT), albumin, bilirubin, gamma-glutamyl transpeptidase (GGT), alpha-feto protein (AFP), urea, and creatinine were performed at baseline (ie, before induction) and every 3–4 months. Blood samples were collected from the jugular vein or auricular vein. Hematology analysis was assessed using an automated blood cell counter, and AST, ALT, albumin, bilirubin, GGT, urea, and creatinine were assessed using enzymatic photometry (Auto Analyzer, BT-3000 plus, Biotechnica, Italy). AFP analysis was conducted using enzyme linked fluorescent assay (ELFA) with automated immunoassay (mini VIDAS, bioMérieux, UK).

Ultrasonography (USG) imaging was conducted using USG Chison TR-8000 with sector and linear probe to monitor liver nodules every few months. All swine were anesthetized for the USG procedure using a combination of ketamine (dose: 20 mg/kg body weight) and xylazine (dose: 2 mg/kg body weight) through intramuscular injection. The procedure was conducted by a team composed of a radiologist or gastrointestinal consultant and a veterinarian with expertise in radiology diagnostics.

Computed tomography (CT) imaging was performed on suspected subjects, yielding positive USG results. The CT scans were conducted using Siemens Somatom CT Simulator 20 slices at Dr. Cipto Mangunkusumo Hospital Jakarta, approximately 60 km from the animal hospital in Bogor, where the swine was maintained. Lopamidol (dose: 1 mL/kg body weight) was used as the contrast medium at an injection rate of 3–4 mL/s. Abdominal CT scans were evaluated in four contrast phases: arterial phase at 15s, early portal at 35s, portal venous at 55s, and 75s after injection.¹⁰ The animals were anesthetized during the procedures. The key criteria of the “wash in and wash out” enhancement pattern were used to diagnose HCC based on CT imaging. Liver tumors were enhanced (“wash in”) in the arterial phase and reduced (“wash out”) in the portal venous phase or equilibrium phase.^{11–13}

Biopsy, Tissue Collection, Histopathological, and Immunohistochemical Evaluation

A biopsy was conducted on animals, and USG screening was performed to confirm the presence of tumor nodules. The biopsy was performed through a disposable, fully automatic biopsy gun under anesthesia using ketamine and xylazine (as described above), with or without the addition of the local anesthetic lidocaine. This procedure was conducted under the guidance of USG. Tumor tissues were also collected during the necropsy procedures. Humane euthanasia was carried out through exsanguination under anesthesia. Prior to all the procedures, the animals were anesthetized to ensure compliance with animal welfare principles.

The tissue samples were fixed in 10% neutral-buffered formalin right away after sacrifice and further processed into paraffin blocks and sectioned at 5 μ m. The sections were then stained using hematoxylin and eosin (HE), reticular, and Masson-Trichrome techniques, and examined under a light microscope. Formalin-fixed tissue sections were employed for the immunohistochemical staining. Heat pretreatment in a decloaking chamber with 10 mM citrate buffer (pH 6.0) at 121°C for 10 minutes was used to retrieve the antigen. Primary antibodies for Hepatocyte Paraffin-1 (Hep Par 1; BioSB,

Santa Barbara, USA; 1:150), Glypican-3 (Biocare Medical, California, USA; 1:100), alpha-fetoprotein (AFP; Zymed, ThermoFisher Scientific, Massachusetts, USA; 1:200), Glutamine Synthetase (Millipore Sigma, California, USA; 1:1000), and Ki-67 (Abcam, Massachusetts, USA; 1:150) were applied to sections for 1 hour at room temperature. The slides were then rinsed in PBS and treated with horseradish peroxidase-conjugated polymer as a secondary antibody for 30 minutes at room temperature, followed by visualization of positive reactions with 3,3-diaminobenzidine (Flexylab Mouse/Rabbit Polyvue HRP DAB Detection Kit, Diagnostic Biosystems, California, USA). Sections were lightly counterstained with hematoxylin. To replace primary antibodies, nonimmunized sera were used as negative controls.

Results

We monitored the body weight of the subjects every week. The domestic swine grew and gained weight rapidly, with a steady increase in body weight observed in each subject. The weight peaked at 14–20 months post-induction (ie, 162–228 kg) and subsequently stabilized or fluctuated (2–6 kg differences, 1.1–3.2% body weight). As shown in Figure 1, the average increase in body weight was lower in the treated swine versus the control subject. We also found that most of the body weights of the ten subjects continued to increase or became stable until the last observation. This trend was also observed in the control animal. Multiple tumor nodules in the liver lobes were discovered during the necropsy (Figure 2).

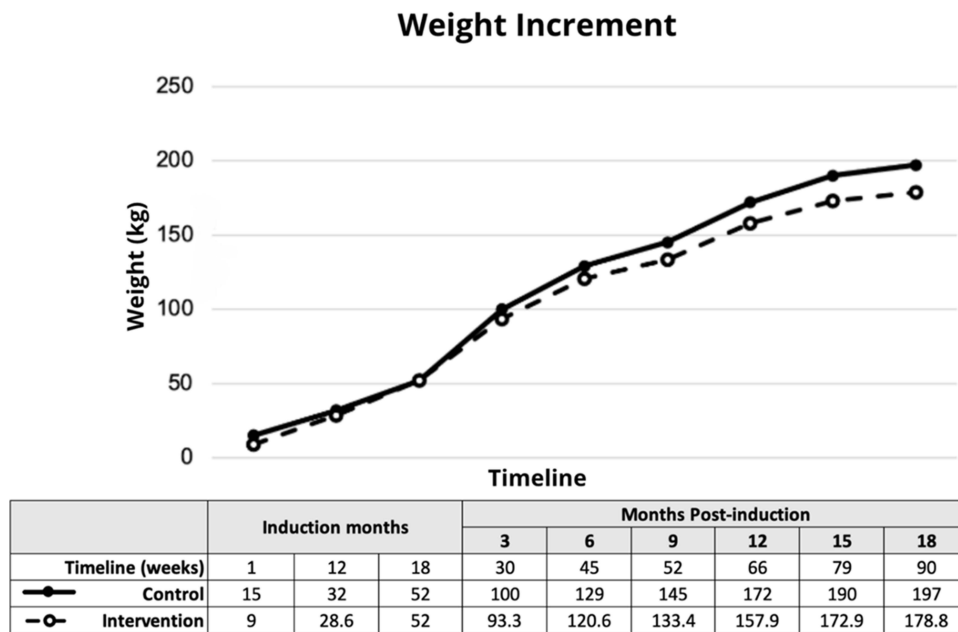


Figure 1 Difference in average weight between the intervention animals (subjects #1–#9) and the control animal #10 (in kg).



Figure 2 Macroscopic observations in the livers of DENA-treated swine. Multiple nodules varying in size were found throughout the liver lobes (a). Small to large, randomly scattered tumor nodules (b) in the right lateral lobe of the liver. A cross-section of a tumor nodule displays a white mass with prominent blood vessels (c). Bar = 5 cm.

Laboratory Testing

The data analysis did not show significant differences between the intervention and control animals at baseline and 18 months, except for an increment in creatinine levels (intervention animals: 1.2 vs 9.1 mg/dL, respectively; control animal: 0.91 vs 0.59 mg/dL, respectively) and AFP (intervention animals: 0.2 vs 11 ng/mL, respectively; control animal: 0.5 vs 8.3 ng/mL, respectively). [Table 1](#) provides a comparison of the laboratory results. Our findings revealed statistically significant differences in thrombocytes, leukocytes, creatinine, urea, and tumor marker AFP at the end of the observation compared with baseline. [Table 2](#) compares laboratory parameters in intervention animals between the baseline and the last observation. Notably, clinically significant differences were observed only in creatinine and urea levels.

Imaging

USG imaging was conducted at 5, 7, 12, and 17 months after induction. In the initial USG examination, suspected tumor nodules were detected in only three (33.3%) subjects (ie, subjects #2, #5, and #9). Biopsies were also performed following the third USG examination in subjects with nodules (ie, subjects #5 and #9). Eventually, the development of liver nodules in the remaining subjects induced with DENA was detected through the fourth USG examination. USG examination could evaluate up to three nodules (size range: 1.2–6.8 cm). In subject #7, assessing the liver through USG was impossible due to abdominal thickness.

CT scans indicated characteristics of “wash in” and “wash out” in some of the tumor nodules examined. As a result, this approach was deemed appropriate for the diagnosis of HCC. Subject #4 was overweight and so could not be evaluated using CT. Subject 7 had a probable mesenteric cyst lesion. However, macroscopic examination revealed that this lesion was normal anatomy; instead, seven tiny nodules (0.3 cm) were discovered in the liver.

In summary, a CT scan evaluated up to 11 tumor nodules in one subject and detected 1.5–6.2 cm nodules. [Table 3](#) describes each subject’s imaging, macroscopic, and histopathology findings in detail. [Figure 3](#) shows the findings of the USG examination, CT scan, and macroscopic evaluation in subject #9.

Macroscopic Findings, Biopsies, Histopathology, and Immunohistochemistry

Necropsy revealed some whitish-yellow nodules in the liver lobes. There were anywhere from 7 to over 100 nodules, ranging in size from 0.5 to 11 cm. There were also a few hemorrhages and distinct blood vessels ([Figure 2](#)). Imaging (USG and CT) revealed fewer tumor nodules in the livers of DENA-treated swine, but macroscopic investigations revealed more. For example, in subject #1, macroscopic analysis found up to seven nodules but USG and CT only detected one. Notably, 30–100 nodules were seen in other subjects suspected of having multiple nodules ([Figure 3](#)).

Subject #2 died nine months after induction from a non-liver cancer-related condition. Despite the discovery of suspicious small nodules with USG, the necropsy, and histopathology revealed high-grade dysplastic nodules rather than HCC.

Individuals #5 and #9 underwent biopsies for suspicious tumor nodules during the third USG examination (ie, 12 months following induction) under USG guidance. The trabecular patterns of hepatocytes were found to be similar to those of dysplastic nodules or well-differentiated HCC. Fifteen months following induction, the two subjects were sacrificed. Histopathological results were re-evaluated, and multiple nodules in both individuals were diagnosed as HCC and hepatic angiosarcoma. [Table 3](#) highlights the research findings for each subject.

[Figure 4](#) describes the histopathological and immunohistochemical evaluations of liver tumor nodules, which showed the presence of HCC and hepatic angiosarcoma in DENA-treated animals. The histopathology of nodular lesions was clearly defined, with hepatocytes organized in a trabecular arrangement. The neoplastic cells generate trabeculae that vary in width; some are small, while others are somewhat thicker; the tumor cells in the liver usually contain 3–10 cell thick trabeculae, minor pleomorphism, and no bile duct proliferation. Those defining many plates of trabeculae thicker than three cells revealed a decrease in reticulin staining among hepatocytes. There were also fibrotic lesions with collagenous fibrous tissue thickening surrounding the cirrhotic nodules. Hepatic angiosarcoma is distinguished by an unencapsulated mass of neoplastic endothelial cells that generate many vascular spaces that are either filled with or empty of erythrocytes. To discriminate between HCC and

Table I Average Laboratory Test Results for the Intervention Animals and Control Animal

Parameters	Normal Value	Baseline		Post Induction		Duration Post-Induction									
						3 Months		6 Months		10 Months		14 Months		18 Months	
		Intervention (n=9)	Control (n=1)	Intervention (n=9)	Control (n=1)	Intervention (n=9)	Control (n=1)	Intervention (n=9)	Control (n=1)	Intervention (n=9)	Control (n=1)	Intervention (n=8)	Control (n=1)	Intervention (n=4)	Control (n=1)
Erythrocytes ($\times 10^6/\mu\text{L}$)	5.0–9.5	5.2	5.7	6.2	7	5.5	4.3	7.1	6.9	7	N/A	6.5	6.9	7.3	7.4
Hemoglobin (g/dL)	9.9–16.5	13.1	12.7	13	13.3	12.2	12.9	13.5	13.1	13.3	N/A	13.3	13.6	14	14.5
Hematocrit (%)	32–50	39.4	39	40.3	42	36.1	38	44.8	44	43.6	N/A	42.1	45	47.3	49
Thrombocytes ($\times 10^3/\mu\text{L}$)	200–700	557.3	333	489.6	448	412	464	386.7	395	413.4	N/A	331.1	169	342.5	299
Leucocytes ($\times 10^3/\text{mL}$)	11.0–22.0	22.2	9.4	12.6	13.1	14.6	13.1	14.7	14.9	11.9	N/A	9.8	7.9	8.6	12.2
ALP (U/L)	97–388	N/A	N/A	356.7	320	202	178	214.1	155	145.9	N/A	76.6	67	168.8	47
SGPT/ALT (U/L)	31–108	73.0	35	67.7	62	53.6	43	48.1	29	66	N/A	54	45	58	49
SGOT/AST (U/L)	25–142	42.8	19	41.3	132	38.7	57	49.8	47	26.8	N/A	54.7	24	35.3	22
Urea (mg/dL)	9.0–31.5	45.2	47.5	33.7	41	37.9	34	34	30	37	N/A	19.1	21	54.4	38.5
Creatinine (mg/dL)	0.6–2.2	1.2	0.91	3.1	4.77	0.8	0.67	3.3	3.41	1.9	N/A	3.8	2.5	9.1	0.59
Albumin (mg/dL)	3.1–48	3.8	3.88	4.1	4.24	3.8	4.17	3.8	4.22	4.2	N/A	4.2	4.3	4.7	3.87
Bilirubin total (mg/dL)	0–0.2	0.9	0.78	0.8	0.76	0.9	0.65	0.4	0.33	0.8	N/A	0.5	0.4	1.8	1.12
Direct (mg/dL)	0.9–3.4	0.3	0.25	0.3	0.36	0.2	0.25	0.2	0.19	0.2	N/A	0.2	0.29	1.3	0.65
Indirect (mg/dL)	0–3.4	0.6	0.53	0.6	0.4	0.6	0.4	0.3	0.14	0.5	N/A	0.3	0.11	0.6	0.47
GGT (U/L)	33–93	50	30	58.3	141	41.2	50	53.8	51	40.8	N/A	48.6	31	49.3	12
AFP (ng/mL)	0–8	0.2	0.5	<0.05	<0.05	<0.5	<0.5	<0.05	<0.05	0.5	N/A	0.5	0.5	11	8.3

Abbreviations: AFP, alpha-fetoprotein; ALP, alkaline phosphatase; ALT, alanine transaminase; AST, aspartate transaminase; GGT, gamma-glutamyl transferase; N/A, not applicable; SGOT, serum glutamic oxaloacetic transaminase; SGPT, serum glutamic pyruvic transaminase.

Table 2 Comparison of Laboratory Parameters of the Intervention Animals at Baseline and Last Observation

Parameter	Baseline (n=9)					Last Observation (n=9)					p-value
	Mean	Median	SD	Min	Max	Mean	Median	SD	Min	Max	
Thrombocytes	557.3	627	162.8	277	730	410.0	353.0	181.7	281.0	882.0	0.015**
Leukocytes	22.2	20.7	3.7	17.3	28.7	9.4	8.5	2.9	6.0	15.2	0.008**
Creatinine	1.2	1	0.5	0.81	1.99	5.7	3.7	7.6	1.0	25.8	0.011**
SGOT	73.0	37	13.5	30	64	56.2	35.0	56.2	17.0	194.0	0.859
GGT	50.0	50	15.6	33	83	45.8	44.0	16.7	20.0	76.0	0.859
Urea*	14.00	11.00	9.50	5.00	36.00	32.44	40.90	12.65	18.00	46.70	0.028**
SGPT*	73.0	71	10.7	56	89	50.4	47.0	13.0	38.0	73.0	0.11
Total bilirubin*	0.9	0.89	0.1	0.86	1.03	0.8	0.6	0.7	0.3	2.5	0.214
AFP*	0.2	0.1	0.2	0.1	0.5	5.6	0.5	6.2	0.5	13.8	0.018**

Notes: *Analysis was conducted using the Wilcoxon test. **p<0.05 indicates statistical significance.

Abbreviations: AFP, alpha-fetoprotein; GGT, gamma-glutamyl transferase; Max, maximum; Min, minimum; SD, standard deviation; SGOT, serum glutamic oxaloacetic transaminase; SGPT, serum glutamic pyruvic transaminase.

benign lesions, we labeled nodular tumors with Hep Par 1, glypican-3, glutamine synthetase, and Ki-67 immunohistochemistry. The cells in the tumor nodules were immunohistochemically positive for Hep Par-1 and Ki-67 but negative for glypican-3 and glutamine synthetase antibodies, indicating that the HCC was early, proliferative, and well differentiated. In addition to histopathology in the liver, there was multi-focal tubular necrosis in the kidney cortex, indicating DENA nephrotoxicity.

Discussion

Conventional domestic swine has been used in this study due to the unavailability of miniature pigs. A miniature pig is a preferred animal model for medical studies owing to its cost-effectiveness, ethical factors, and biological characteristics that resemble the human anatomy, physiology, pathophysiology, and disease course.¹⁴ However, miniature pigs are not readily available in Indonesia. Hence, full-sized farm-breed domestic swine were used to conduct the present study. In 1977, Graw et al investigated the use of swine models to induce HCC with DENA for the first time, using Gottingen miniature pigs.¹⁵ Subsequently, research studies continued to explore methods that could be utilized to enhance the carcinogenic effect. Li et al, using China Taihu pigs, was the first to introduce the intraperitoneal administration of DENA for the induction of HCC, resulting in a faster response than oral administration.¹⁶ This method was also conducted in other studies using Yucatan miniature pigs, with the addition of PB as an accelerator of carcinogenesis.^{6,17} DENA is an established hepatocarcinogen naturally present in a variety of foods. It induces hepatocarcinogenesis by forming alkyl DNA adducts, DNA structure alteration, chromosomal aberrations, micronuclei induction, and oxidative stress.¹⁸ DENA can be administered via several routes, namely peritoneal injection, oral gavage, or gaseous inhalation.

A previous study with DENA-treated conventional domestic swine produced only mesenchymal tumors (hepatic angiosarcoma and leiomyoma) with no progression to HCC; the study used repeated DENA treatments without PB.¹⁹ To the best of our knowledge, this is the first study using full-sized farm breed (conventional) domestic swine to induce HCC by administering DENA and PB. The successful induction of HCC in our study may be a milestone for other investigators aiming to develop large-animal models for medical research using widely available domestic swine. Compared with the induction of HCC in the miniature pig study conducted by Ho et al, the present study yielded similar results regarding detecting suspected tumor nodules by imaging (ie, at 5–11 months vs 5–17 months, respectively). Nevertheless, the present analysis revealed a slightly longer latency period for the pathologic results (ie, initiated at 10–18 months vs 15–22 months, respectively).⁶ The first pig (subject #2) expired nine months post-induction; however, based on the pathological examination, the suspected nodule was not HCC. Hence, a longer latency period may be required for detecting HCC. In our investigation, the latency period was initiated at 15 months post-induction. The longer latency period observed in our study might be attributed to the larger species than miniature pigs. Despite using younger animals at the time of induction (age: 2 months) and the addition of PB, the tumor latency period was not

Table 3 Radiologic, Macroscopic, and Histopathological Findings of the Subjects

Subject	Sex	Imaging Findings				Macroscopic Findings	Histopathology	
		Ultrasonography (Duration Post-Induction)			CT scan			
		1st (5 Months)	2nd (7 Months)	3rd (12 Months)				4th (17 Months)
#1	Male	No abnormalities found			Suspected tumor nodule: 2.8 cm	Single solid hypodense nodule: 2.6 cm	Nodule approximately 2.5 cm with liquefactive necrosis; and up to 7 tumor nodules: <0.3–0.5 cm	HCC
#2	Male	Suspected tumor nodule: 2.7 cm	Suspected tumor nodule: 6.5 cm		Expired	N/A	Normal liver, no tumor nodules (at 9 month post-induction)	Dysplastic nodules Fibrosis
#3	Female	No abnormalities found			Suspected tumor nodule: 1.8 cm	Two hypodense nodules: 2.9 and 2.2 cm	Multiple tumor nodules; largest diameter: 6 cm; enlarged lymph nodes	HCC, HA Cirrhosis
#4	Male	No abnormalities found			Two suspected tumor nodules: 2.4 and 1.9 cm	N/A (subject weight: >225 kg, not suitable for CT scan couch)	Multiple tumor nodules (up to 34); largest diameter: 4.5 cm; enlarged lymph nodes	HCC, HA Cirrhosis
#5	Male	3 tumor nodules: 1.6–2 cm	Suspected tumor nodule: 5 cm	Suspected tumor nodule: 1.6 cm	Expired	N/A	Multiple tumor nodules (up to 80); largest diameter: 7 cm	HCC, HA Cirrhosis
#6	Male	No abnormalities found			Suspected tumor nodule: 3 cm	Multiple solid hypodense nodules (up to 11); largest diameter: 5.1 cm; observed widely in homogenous liver parenchyma	Multiple tumor nodules (up to 100); largest diameter: 12 cm; enlarged lymph nodes	HCC, HA Cirrhosis
#7	Male	No abnormalities found			Not detected; difficult to observe, liver excessively deep for observation	Mesenteric cyst lesion: 6.2×4.9 cm	7 small tumor nodules: ±0.3 mm in liver; enlarged lymph nodes	HCC Cirrhosis
#8	Female	No abnormalities found			Suspected tumor nodule: 2.8 cm	Single solid hypodense nodule: 2.5 cm	Multiple tumor nodules (up to 28); largest diameter: 3 cm	HCC, HA Cirrhosis
#9	Female	Single tumor nodule: 1.2 cm	No abnormalities found	Suspected tumor nodule: 5.6 cm	Expired	Multiple solid tumor hypodense nodules (up to 10): 1.5–6.2 cm; single cyst lesion: 1.8 cm	Multiple tumor nodules (up to 40); largest diameter: 5.5 cm; enlarged lymph nodes	HCC, HA Cirrhosis
#10	Male	No abnormalities found				N/A	Normal liver	Normal liver

Notes: Data from CT scans and macroscopic findings were collected within 6–22 and 15–22 months after induction, respectively. Subject 2#: expired at week 56 (ie, 9 months post-induction) due to reasons not related to liver cancer (necropsy); Subject 5#: sacrificed at week 79; Subject #9: sacrificed at week 83; Subject #7: sacrificed at week 89; Subject #8: sacrificed at week 91; Subject #6: sacrificed at week 93; Subject #3: sacrificed at week 107; Subject #3: sacrificed at week 108; Subjects #1, #4, and #10: sacrificed at week 110.

Abbreviations: CT, computed tomography; DENA, N-diethylnitrosamine; HCC, hepatocellular carcinoma; HA, hepatic angiosarcoma; N/A, not applicable; PB, phenobarbital.

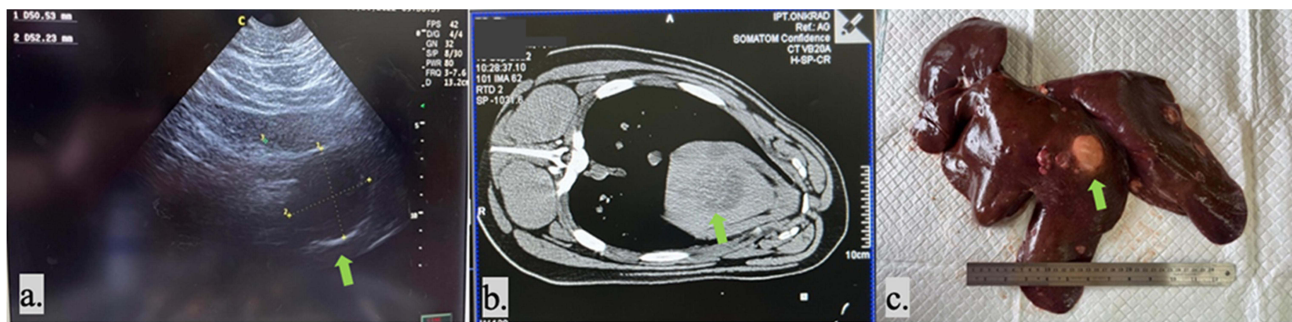


Figure 3 These figures depict the correlation between (a) Ultrasonography, (b) Computed tomography (CT) scan, and (c) Macroscopic findings. Green arrows indicate a solitary tumor found in subject #9 of DENA-treated swine using ultrasonography, CT scan, and macroscopic examination, respectively.

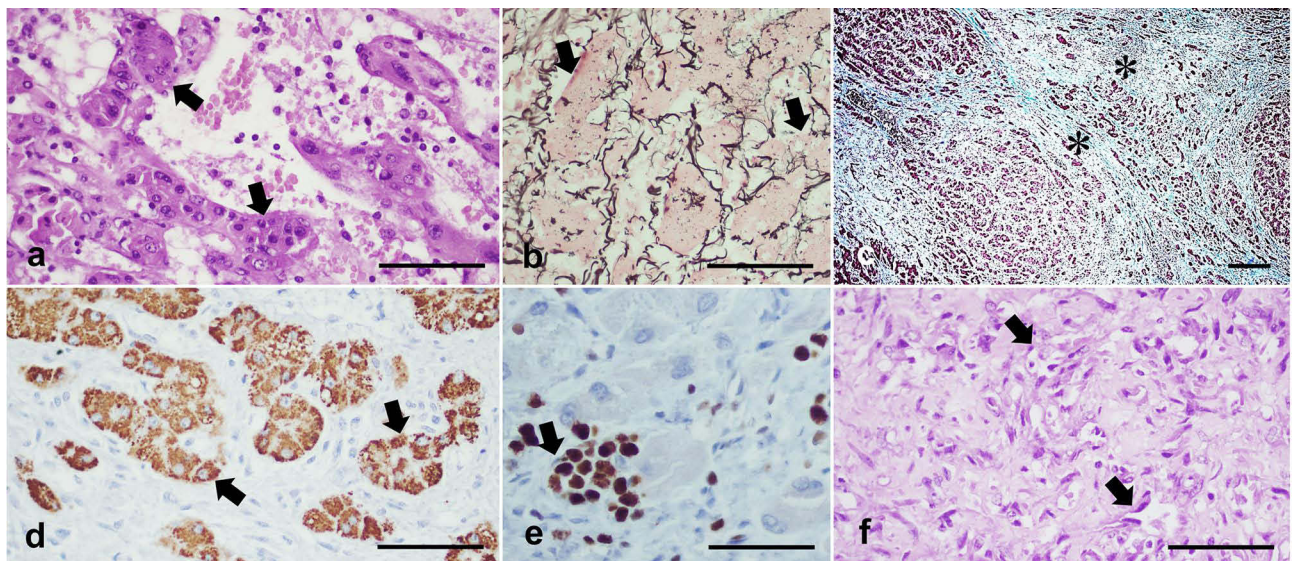


Figure 4 Histopathological and immunohistochemical assessments of tumors in DENA-treated animals. Hematoxylin-and-eosin (HE) evaluation in (a) showing trabecular pattern of HCC composed of variably thick trabeculae formed by neoplastic hepatocytes separated by vascular channels of various widths. Some trabeculae in this case are two cells thick and in other regions the hepatocytes pile together to form variably thick trabeculae (arrows). There are small foci of reticulin loss (arrows) among hepatocyte plates (b) in reticulin staining slide. Masson-Trichrome staining (c) revealed thick collagenous fibrous bundles (asterisks) surrounding the cirrhotic nodules in DENA-treated liver. Immunostaining of Hep Par-1 (d) intensely positive in trabeculae of tumor cells (arrows). A Ki-67 immunostaining (e) shows an increased proliferative rate in the liver of DENA-treated swine (arrow). A HE section of hepatic angiosarcoma (f) shows a densely cellular neoplasm made up of spindle cells that form different diameters of blood vessels. Bar = 50 μ m.

shortened in our study compared with the other research. The involvement of young animals was necessary to produce a swine model for radiotherapy that avoids the rapid increment in body weight, which could potentially exceed the weight limit of the weighing machine (ie, 200 kg).

The results of this study demonstrated an increment in the weight of domestic swine, thereby depicting their rapid growth following induction and during the carcinogenesis phase. These data were minimal. Therefore, this evidence could be helpful as a reference or example for future studies since the weight of swine might exceed the maximum weight limit of specific weighing machines. Moreover, higher body weights complicate the handling and transportation of animals. Based on the findings of our study, the tumors appeared after the animals reached a weight ranging from 160 to 228 kg. A comparison of all animal studies performed thus far using pigs for the induction of liver tumors is shown in Table 4.

Laboratory monitoring indicated that the parameters of routine blood tests and liver function tests did not change significantly from baseline. Serum AFP is a biomarker commonly used to diagnose HCC and monitor treatment response. Elevating serum AFP levels (ie, >400 ng/mL) highly suggest HCC.²⁰ In our study, the levels of AFP did not exceed the

Table 4 Comparison of Other Studies Involving Swine Models of DENA-Induced HCC

Author, Year	Species	N	Sex	Chemical Substances, Doses	Route of Administration	Age at Treatment (Months)	Imaging	Lesion Latency by Imaging (Months)	Tumor Latency (By Pathology)	Liver Pathology Findings
Graw, 1977 ¹⁵	Gottingen minipig	6	Unknown	DENA 0.4 mg/kg	Per os	6	None	None	3–5 years, HCC, HA, sarcoma	Cirrhosis, fibrosis, necrosis
Li, 2006 ¹⁶	China Taihu	6	4 males, 2 females	DENA 10 mg/kg	i.p.	3	CT, MRI	10–12	10–12 months, HCC	Normal
Mitchell, 2016 ¹⁷	Yucatan minipig	8	Female	DENA 15 mg/kg	i.p.	3	CT	9–15	16–27 months, HCC, HA, sarcoma	Cirrhosis, fibrosis
Ho, 2017 ⁶	Yucatan minipig	11	Female	DENA 15 mg/kg + PB 3–5 mg/kg	DENA: i.p.; PB: per os	6	MRT	5–11	10–18 months, HCC, HA, FNH, fibrotic lesions	Normal
Kessler, 2019 ¹⁹	Domestic swine	6	3 males, 3 females	DENA 15 or 30 or 50 mg/kg weekly or every 2 weeks, or 200 mg/kg single dose	i.p.	–	CT	Not specifically reported	284–365 days (~9–12 months)	Hepatic angiosarcoma
Present study	Domestic swine	10	7 males, 3 females	DENA 15 mg/kg + PB 3–5 mg/kg	DENA: i.p.; PB: per os	2	USG, CT	5–17	15–22 months, HCC, HA	Cirrhosis, Fibrosis

Abbreviations: CT, computed tomography; DENA, N-diethylnitrosamine; FNH, focal nodular hyperplasia; HA, hepatocellular adenoma; HCC, hepatocellular carcinoma; HA, hepatic angiosarcoma; i.p., intraperitoneal; MRI, magnetic resonance imaging; MRT, magnetic resonance tomography; N/A, not applicable; PB, phenobarbital; USG, ultrasonography.

threshold for HCC at any point. Importantly, even when the necropsy results revealed the presence of multiple tumor nodules in all lobes, the blood parameters of liver function remained within the standard limit. A possible explanation for this finding may be the presence of sufficient remnant healthy tissues in the liver to perform its function. It has been reported in humans that as low as 20–30% of the total liver volume is sufficient to maintain liver function.²¹

The creatinine and urea levels were higher at the last laboratory examination than at the baseline. The mean creatinine levels were also higher in the intervention animals compared with the control animals (intervention animals: 9.1 mg/dL at 18 months vs 1.2 mg/dL at baseline; control animals: 0.91 mg/dL at 18 months vs 0.59 mg/dL at baseline). These findings are statistically and clinically significant since creatinine and urea levels could explain renal damage in this study. Additionally, multiple tubular necrosis in the histopathology of the kidney supports DENA nephrotoxicity. Elguindy et al²² and Vargas-Olvera et al²³ reported that the administration of DENA significantly altered kidney function in mice by elevating serum urea and creatinine levels, indicative of renal damage.^{22,23} DENA administration induces oxidative stress and reactive oxygen species attack on mesangial and endothelial cells, thereby altering the structure and function of the glomerulus and further inducing kidney cell injury.²³

Owing to its ease of operation, real-time results, non-invasiveness, and portability, USG is the most commonly used liver imaging method in clinical practice. In this study, USG imaging was completed every 2–5 months. However, the USG examination is an operator-dependent procedure; hence, experts should perform it. The thickness of swine skin and fat layers poses another challenge to the use of USG. Domestic swine exhibited a rapid increment in body weight, reaching a peak of 160–225 kg. This increase impaired our ability to observe some parts of the liver entirely in depth. Moreover, considering the limitation of our USG device and its probe, detecting nodules in the liver became difficult. This might explain some inconsistencies in the recorded size of nodules. However, it is possible to conduct biopsies through USG guidance.

Dynamic contrast-enhanced CT scans and multimodal magnetic resonance imaging (MRI) scans are the preferred imaging methods for diagnosing HCC.²⁴ This study showed that CT is more effective than USG in detecting tumor nodules. CT scans could detect more tumor nodules than USG (eg, 11 vs one nodule in subject #6) and could detect limited to three nodules (subject #5). Nonetheless, a phenomenon termed “iceberg” occurred, in which the reported number of tumor nodules detected through imaging is markedly lower than that discovered during the necropsy. In one subject, >30 or even 100 small tumor nodules were detected (average diameter: 0.3–2 cm). This finding may be due to the limitation of CT to detect such small lesions. MRI detects smaller liver tumors (diameter: <2.0 cm) more effectively than CT imaging.^{24,25} Furthermore, detecting liver tumors with a size <1 cm involves using the hepatocyte-specific MRI contrast agent gadoxetic acid disodium.^{26,27}

In the present study, administering DENA through intraperitoneal injection led to the development of multiple nodules in all swine’s livers. Further pathological examination revealed the presence of two different malignancies, namely HCC and hepatic angiosarcoma. Various tumor entities following DENA-induced carcinogenesis have also been found in other studies, such as those conducted by Graw et al, Mitchell et al, and Ho et al.^{6,15,17} In those studies, the second tumor entity was typically sarcoma.

The current study’s tumor histopathology, notably the trabecular type of HCC and hepatic angiosarcoma, is consistent with prior findings in DENA-treated swine.^{6,19} All of the HCCs detected in the current investigation were well differentiated rather than poorly differentiated, implying that dysplastic alterations progressed throughout time rather than becoming de novo carcinoma.^{6,28} The high levels of immunopositivity for Hep Par-1, which reveals both normal and malignant hepatocytes, and Ki-67, which demonstrates cell proliferation, are consistent with earlier research on HCC in DENA-treated swine.¹⁶ Our findings did not indicate immunopositivity to Glypican-3 or AFP, which is consistent with earlier findings of well-differentiated HCC in many cases.^{6,28,29} AFP and glypican-3 levels may not consistently indicate positivity during the initial phases of well-differentiated and chemically induced hepatocellular carcinoma (HCC). This is due to the limited sensitivity and specificity of AFP and glypican-3 in detecting early-stage HCC.^{28,29}

Our observation demonstrated the eventual appearance of tumor nodules as time progressed. At the initial USG screening (ie, at five months post-induction), suspicious nodules were detected in only three subjects. However, during the last USG screening performed 17 months after induction, the remaining intervention subjects without previously visible tumors had eventually developed nodules. In total, eight of nine subjects that received DENA developed tumor

nodules, which were confirmed pathologically. Only one subject expired at week 56 (ie, nine months post-induction), thereby not allowing the exhibit of the final carcinogenesis result at the end of the investigation. The first confirmed case of HCC in this study was found after 15 months.

Limitations of the Study

In our animal model, the actual timing of HCC development is not precisely known. This limitation is due to the lack of imaging equipment for screening and diagnosing tumor nodules in the liver. Our facility does not have any CT or MRI equipment. Consequently, the screening for liver nodules was performed using a USG device, which is characterized by several limitations compared with CT or MRI. Thus, more frequent screening and better imaging modalities (eg, MRI) are warranted to more accurately determine the actual timing of HCC development in future studies. Due to the small number of subjects included in this study, the power of the statistical analysis is limited.

Conclusion

In this investigation, we successfully produced a swine model with HCC induced by the genotoxic agent DENA. The administration of DENA and PB in pigs was effective, though a long time was required to develop HCC in domestic pigs versus minipigs (ie, 15–22 months). The use of younger swine did not shorten the latency period previously reported in similar studies. The choice of imaging modality may affect the prompt diagnosis of HCC. The discrepancy in the detection of tumor nodules between USG, CT, or macroscopic findings was associated with the size of the tumors and the sensitivity and specificity of the modality used. Moreover, the present approach can induce more than one type of cancer; in this study, the detected malignancies were HCC and hepatic angiosarcoma. This study demonstrates that the liver in swine treated with DENA exhibits gross characteristics, histopathology, and immunohistochemistry results that closely resemble those of early, well-differentiated hepatocellular carcinoma (HCC) in humans.

Acknowledgments

We thank Prof. Dr. Drh. Gunanti, MS, Executive Director of IPB Veterinary Teaching Hospital, Bogor, Indonesia, for approving this study to be conducted at the animal hospital of IPB University. We also thank Drh. Arni Diana Fitri, M.Si for helping with the maintenance and monitoring of the animals throughout the study. We thank Dr. I Wayan Murna, Sp. Rad (K) and Dr. Benny Zulkarnaen, Sp.Rad (K) for their valuable contributions as radiology experts.

Funding

This study was partly funded by the PUTI grant for the Doctoral Scheme of Universitas Indonesia (grant number: BA-756/UN2.RST/PPM.00.03.01/2020). The grant was used to purchase the animals and DENA.

Disclosure

The authors report no conflicts of interest in this work.

References

1. Sung H, Ferlay J, Siegel RL, et al. Global cancer statistics 2020: GLOBOCAN estimates of incidence and mortality worldwide for 36 cancers in 185 countries. *CA Cancer J Clin.* 2021;71(3):209–249. doi:10.3322/caac.21660
2. Raza A. Hepatocellular carcinoma review: current treatment, and evidence-based medicine. *World J Gastroenterol.* 2014;20(15):4115. doi:10.3748/wjg.v20.i15.4115
3. El-Serag HB. Hepatocellular carcinoma. *N Engl J Med.* 2011;365(12):1118–1127. doi:10.1056/NEJMra1001683
4. Zhang HE, Henderson JM, Gorrell MD. Animal models for hepatocellular carcinoma. *Biochim Biophys Acta Mol Basis Dis.* 2019;1865(5):993–1002. doi:10.1016/j.bbadis.2018.08.009
5. Tolba R, Kraus T, Liedtke C, Schwarz M, Weiskirchen R. Diethylnitrosamine (DEN)-induced carcinogenic liver injury in mice. *Lab Anim.* 2015;49(1_suppl):59–69. doi:10.1177/0023677215570086
6. Ho J, Ware M, Law J, et al. Improved, shorter-latency carcinogen-induced hepatocellular carcinoma model in pigs. *Oncology.* 2018;95(6):360–369. doi:10.1159/000491092
7. Weisburger JH, Griswold DP, Prejean JD, Casey AE, Wood HB, Weisburger EK. The carcinogenic properties of some of the principal drugs Used in clinical cancer chemotherapy. In: *The Ambivalence of Cytostatic Therapy.* Berlin, Heidelberg: Springer Berlin Heidelberg; 1975:1–17. doi:10.1007/978-3-642-80940-8_1

8. Hori T, Yokobori K, Moore R, Negishi M, Sueyoshi T. CAR requires Gadd45 β to promote phenobarbital-induced mouse liver tumors in the early stage. *Front Oncol.* 2023;13. doi:10.3389/fonc.2023.1217847
9. Butterworth KT, Williams JP. Animal models for radiotherapy research: all (animal) models are wrong but some are useful. *Cancers.* 2021;13(6):1319. doi:10.3390/cancers13061319
10. Bekheit M, Bucur PO, Wartenberg M, Vibert E. Computerized tomography-based anatomic description of the porcine liver. *J Surg Res.* 2017;210:223–230. doi:10.1016/j.jss.2016.11.004
11. Omata M, Cheng AL, Kokudo N, et al. Asia-Pacific clinical practice guidelines on the management of hepatocellular carcinoma: a 2017 update. *Hepatol Int.* 2017;11(4):317–370. doi:10.1007/s12072-017-9799-9
12. Marrero JA, Kulik LM, Sirlin CB, et al. Diagnosis, staging, and management of hepatocellular carcinoma: 2018 practice guidance by the American Association for the Study of Liver Diseases. *Hepatology.* 2018;68(2):723–750. doi:10.1002/hep.29913
13. Galle PR, Forner A, Llovet JM, et al. EASL clinical practice guidelines: management of hepatocellular carcinoma. *J Hepatol.* 2018;69(1):182–236. doi:10.1016/j.jhep.2018.03.019
14. Wang S, Liu Y, Fang D, Shi S. The miniature pig: a useful large animal model for dental and orofacial research. *Oral Dis.* 2007;13(6):530–537. doi:10.1111/j.1601-0825.2006.01337.x
15. Graw JJ, Berg H. Hepatocarcinogenic effect of DENA in pigs. *Zeitschrift für Krebsforschung und Klinische Onkologie.* 1977;89(2):137–143. doi:10.1007/BF00308514
16. Li X, Zhou X, Guan Y, Wang YXJ, Scutt D, Gong QY. N-Nitrosodiethylamine-induced pig liver hepatocellular carcinoma model: radiological and histopathological studies. *Cardiovasc Intervent Radiol.* 2006;29(3):420–428. doi:10.1007/s00270-005-0099-8
17. Mitchell J, Tinkey PT, Avritscher R, et al. Validation of a preclinical model of Diethylnitrosamine-induced hepatic neoplasia in Yucatan miniature pigs. *Oncology.* 2016;91(2):90–100. doi:10.1159/000446074
18. Mahmoud AM, Zaki AR, Hassan ME, Mostafa-Hedeab G. Commiphora molmol resin attenuates diethylnitrosamine/phenobarbital-induced hepatocarcinogenesis by modulating oxidative stress, inflammation, angiogenesis, and Nrf2/ARE/HO-1 signaling. *Chem Biol Interact.* 2017;270:41–50. doi:10.1016/j.cbi.2017.04.012
19. Kessler SM, Lebber B, Hopstädter J, et al. Diethylnitrosamine (DENA) recapitulates the formation of hepatic angiosarcoma in pigs. *PLoS One.* 2019;14(5):e0214756. doi:10.1371/journal.pone.0214756
20. Zhou J, Sun H, Wang Z, et al. Guidelines for the diagnosis and treatment of hepatocellular carcinoma (2019 edition). *Liver Cancer.* 2020;9(6):682–720. doi:10.1159/000509424
21. Guglielmi A, Ruzzenente A, Conci S, Valdegamberi A, Iacono C. How much remnant is enough in liver resection? *Dig Surg.* 2012;29(1):6–17. doi:10.1159/000335713
22. Elguindy NM, Yacout GA, El Azab EF. Amelioration of DENA-induced oxidative stress in rat kidney and brain by the essential oil of *Elettaria cardamomum*. *Beni Suef Univ J Basic Appl Sci.* 2018;7(3):299–305. doi:10.1016/j.bjbas.2018.02.005
23. Vargas-Olvera CY, Sánchez-González DJ, Solano JD, et al. Characterization of N-diethylnitrosamine-initiated and ferric nitrilotriacetate-promoted renal cell carcinoma experimental model and effect of a tamarind seed extract against acute nephrotoxicity and carcinogenesis. *Mol Cell Biochem.* 2012;369(1–2):105–117. doi:10.1007/s11010-012-1373-0
24. Lee YJ, Lee JM, Lee JS, et al. Hepatocellular carcinoma: diagnostic performance of multidetector CT and MR imaging—a systematic review and meta-analysis. *Radiology.* 2015;275(1):97–109. doi:10.1148/radiol.14140690
25. Liu X, Jiang H, Chen J, Zhou Y, Huang Z, Song B. Gadoteric acid disodium-enhanced magnetic resonance imaging outperformed multidetector computed tomography in diagnosing small hepatocellular carcinoma: a meta-analysis. *Liver Transpl.* 2017;23(12):1505–1518. doi:10.1002/lt.24867
26. Yoo SH, Choi JY, Jang JW, et al. Gd-EOB-DTPA-enhanced MRI is better than MDCT in decision-making of curative treatment for hepatocellular carcinoma. *Ann Surg Oncol.* 2013;20(9):2893–2900. doi:10.1245/s10434-013-3001-y
27. Ding Y, Chen CZ, Rao SX, Zeng MS. A compared study on Gd+-EOB-DTPA and Gd+-DTPA-enhanced MRI in the detection of hepatocellular carcinoma. *Chin J Gen Surg.* 2013;28(9):682–685. doi:10.3760/cma.j.issn.1007-631X.2013.09.010
28. Shafizadeh N, Ferrell LD, Kakar S. Utility and limitations of glypican-3 expression for the diagnosis of hepatocellular carcinoma at both ends of the differentiation spectrum. *Mod Pathol.* 2008;21:1011–1018. doi:10.1038/modpathol.2008.85
29. Wang T, Zhang K. New blood biomarkers for the diagnosis of AFP-negative hepatocellular carcinoma. *Front Oncol.* 2020;10:1316. doi:10.3389/fonc.2020.01316

Cancer Management and Research

Dovepress

Publish your work in this journal

Cancer Management and Research is an international, peer-reviewed open access journal focusing on cancer research and the optimal use of preventative and integrated treatment interventions to achieve improved outcomes, enhanced survival and quality of life for the cancer patient. The manuscript management system is completely online and includes a very quick and fair peer-review system, which is all easy to use. Visit <http://www.dovepress.com/testimonials.php> to read real quotes from published authors.

Submit your manuscript here: <https://www.dovepress.com/cancer-management-and-research-journal>